ACCEPTED MANUSCRIPT

Cortical recruitment and functional dynamics in postural control adaptation and habituation during vibratory proprioceptive stimulation

To cite this article before publication: Kyle Joseph Edmunds *et al* 2019 *J. Neural Eng.* in press https://doi.org/10.1088/1741-2552/ab0678

1
2
3
4
5
6
7
8
9
10
11
12
13
14
15

Cortical recruitment and functional dynamics in postural control adaptation and habituation during vibratory proprioceptive stimulation

KJ Edmunds[1], H Petersen[2,3], M Hassan[4], S Yassine[4], A Olivieri[5], F Barollo[1,6], R Friðriksdóttir[1], P Edmunds[1], MK Gíslason[1], A Fratini[6], and P Gargiulo[1,7]

[1]Institute for Biomedical and Neural Engineering, Reykjavík University, Reykjavík, Iceland
[2]Department of Anatomy, University of Iceland, Reykjavík, Iceland
[3]Akureyri Hospital, Akureyri, Iceland
[4]University of Rennes, LTSI - U1099, F-35000 Rennes, France
[5]Dept. of Electrical Eng. and Information Tech., University of Naples Federico II, Naples, Italy
[6]School of Life and Health Sciences, Aston University, Birmingham, UK
[7]Department of Science, Landspítali, Reykjavík, Iceland

7/9/2018

1   **Address for Correspondence:**

2

3   *Dr. Kyle J. Edmunds*

4   Institute for Biomedical and Neural Engineering, Reykjavík University

5   Menntavegur 1, 101 Reykjavík, Iceland

6   +354 788 9320

7   Email: kyle14@ru.is

8

9   **-Abstract**

10   ***Objective.*** Maintaining upright posture is a complex task governed by the integration of afferent
11   sensorimotor and visual information with compensatory neuromuscular reactions. The objective of
12   the present work was to characterize the visual dependency and functional dynamics of cortical
13   activation during postural control.

14   ***Approach.*** Proprioceptic vibratory stimulation of calf muscles at 85 Hz was performed to evoke
15   postural perturbation in open-eye (OE) and closed-eye (CE) experimental trials, with pseudorandom
16   binary stimulation phases divided into four segments of 16 stimuli. 64-channel EEG was recorded at
17   512 Hz, with perturbation epochs defined using bipolar electrodes placed proximal to each vibrator.
18   Power spectra variation and linearity analysis was performed via fast Fourier transformation into six
19   frequency bands (Δ, 0.5-3.5 Hz; θ, 3.5-7.5 Hz; α, 7.5-12.5 Hz; β, 12.5-30 Hz; γ_{low}, 30-50 Hz; and γ_{high},
20   50-80 Hz). Finally, functional connectivity assessment was explored via network segregation and
21   integration analyses.

22   ***Main Results.*** Spectra variation showed waveform and vision-dependent activation within cortical
23   regions specific to both postural adaptation and habituation. Generalized spectral variation yielded
24   significant shifts from low to high frequencies in CE adaptation trials, with overall activity suppressed
25   in habituation; OE trials showed the opposite phenomenon, with both adaptation and habituation
26   yielding increases in spectral power. Finally, our analysis of functional dynamics reveals novel cortical
27   networks implicated in postural control using EEG source-space brain networks. In particular, our
28   reported significant increase in local θ connectivity may signify the planning of corrective steps and/or
29   the analysis of falling consequences, while α band network integration results reflect an inhibition of
30   error detection within the cingulate cortex, likely due to habituation.

31   ***Significance.*** Our findings principally suggest that specific cortical waveforms are dependent upon the
32   availability of visual feedback, and we furthermore present the first evidence that local and global brain
33   networks undergo characteristic modification during postural control.

34   ***Keywords: Vertical Posture, Proprioceptive Stimulation, EEG, Power Spectral Density, Functional***
35   ***Connectivity***

36

1. Introduction

Maintaining upright posture is a complex task governed by the integration of afferent sensorimotor information with compensatory neuromuscular reactions [1], and the compensation for unpredictable perturbations in balance is essential to retaining stability and avoiding injury from falling. The cerebral cortex and central nervous system (CNS) play integral roles in postural control, incorporating information from visual, somatosensory, and vestibular systems to carry out the corrective motions needed to maintain balance [2-4]. The role of the CNS and subcortical structures in this regard is well-documented in literature for the innate generation of feedforward and feedback adaptive adjustments to reduce the risk of balance loss [5-7]. However, understanding the role of the cerebral cortex has been of comparatively recent focus, along with its potential relationship with visual subsystems. Nonetheless, there is growing evidence for the importance of cortical involvement in adapting to transient balance perturbation [4-6, 8-13].

1.1.   Role of the Cerebral Cortex in the Postural Control System

The contributions from infratentorial or supratentorial structures in maintaining upright posture has been of much recent focus in vestibular research involving human postural biomechanics. In such studies, postural control feedback is generalized under single inverted pendulum (SIP) theory, wherein the simplest spinal model (containing one or few spinal segments) is subjected to reflex controls aimed at maintaining a constant body center of pressure (COP) on a limited base of support [14-16]. This SIP model has been shown to accurately represent postural control during both small body perturbations inherent to bipedal quiet stance [17], as well as movement when the body is sufficiently far from its limits of antero-posterior or medial-lateral stability [18]. In general, when upright stance is perturbed, infratentorial reflexes trigger synchronized, efferent muscle reactions within the spine; these reflexes are commensurately registered by supratentorial (cortical) structures. This combination of feedback systems during postural perturbation is a complex relationship that further involves central and

3

61　peripheral nervous structures [20]; as such, optimizing the validity of extant postural control models

62　presents a strategic priority for research [19-21].

63　Characterizing the precise role of the cerebral cortex in governing the supratentorial response to

64　postural perturbation has been addressed by research on sensorimotor integration, which has

65　specifically implicated the posterior-parietal cortex for its interconnectivity with motor and premotor

66　cortices [2, 22], and further studies have suggested the region's role in complex sensorimotor

67　processing [23-25]. In addition, enhanced activation of the fronto-central region has been reported

68　during the visual recognition of one's postural instability, both with and without warning cues [4, 5,

69　26], as well as during self-initiated postural changes [6, 13, 27]. In particular, the anterior cingulate

70　cortex (ACC) in the fronto-central region is well-known for its crucial involvement in action monitoring

71　and the detection of error signals, specifically increasing in activity during the detection of balance

72　instability [28-30].

73　While many tools have been employed to study neurocognitive processes in this regard, the use of

74　electroencephalography (EEG) as a neuroimaging technique remains disparately reported.

75　Nonetheless, extant literature has investigated the utility of EEG through examination of evoked

76　potentials associated to balance perturbation. Most typically, changes in evoked activity have been

77　reported as time-domain event-related potentials (ERP) and/or perturbation-evoked responses (PER),

78　and ERP/PER components such as N1 amplitudes and Contingent Negative Variation (CNV) have been

79　reported [4-6, 12, 13]. While ERP responses have exhibited a wide distribution during unpredictable

80　perturbations to upright posture, the propensity of literature suggests the generalizability of responses

81　to fronto-central and occipital sites [59-61]. Power spectral density (PSD) analysis represents an

82　alternative, yet analogously conventional method for EEG signal analysis, which remains comparatively

83　underreported in postural control literature, despite its proven utility in cognitive and/or motor task

84　EEG studies [28, 31-33].

4

85 In addition to ERP analysis, emerging evidence highlights the utility of EEG for the estimation of

86 functional brain network dynamics; indeed, functional connectivity in this regard plays a crucial role in

87 many cognitive and motor functions [34]. In addition to its non-invasiveness and the relative ease of

88 use (portability), a key advantage of EEG in discerning functional neural connectivity is its excellent

89 temporal resolution, which offers the unique opportunity to both track large-scale brain networks over

90 very short durations and to analyze fast dynamic changes that can occur during resting states or in

91 brain disorders [35].

92 **1.2.   Comparative Indicators for the Cortical Response: Adaptation and Habituation**

93 There are two primary indicators for cortical response in balance perturbation and postural control:

94 cortical *adaptation* and *habituation*. Cortical adaptation in postural control may be described as

95 transient changes in motor control strategy when exposed to acute changes in balance or sensorimotor

96 input [36]. Cortical habituation, conversely, may be defined as the process of gradual improvement in

97 postural rescue acquired through repetitive adaptation, through which enhanced motor control is

98 acquired from repetitive, strategic corrections [37, 38]. Indeed, the contributory mechanisms of

99 vestibular and subcortical systems represent phylogenically older structures for governing balance and

100 employing learned motor movements, altogether suggesting their comparatively larger roles in

101 postural adaptation [39]. In general, postural control is transiently and longitudinally improved by

102 repetitive exposure to postural perturbation, such as in daily exercise, which encourages both

103 functional and structural adaptation in the neuromuscular system [31, 40, 41]. In a research context,

104 external vibratory stimulation applied to a muscle or tendon is a typical technique for the artificial

105 induction of postural change, evoking the activation of proximal muscles to instigate an erroneous

106 sensation of movement, which ultimately induces a commensurate postural response [33, 42].

107 Maintaining vertical posture may be generalized by the complex integration of feed-forward and feed-

108 back mechanisms in cortical and subcortical structures to generate forces toward a supporting surface;

109 this is typically achieved by calculated adjustments to the position of body segments or extremities.

5

110   However, the precise role of the cerebral cortex and functional dynamics during the adaptation or

111   influence of motor neuron executions remains debated; to our knowledge, there exists no study on

112   the assessment of changes in EEG power spectra and functional connectivity during proprioceptic

113   stimulation. Furthermore, while vision has been known to play an important role in postural control,

114   its relationship with cortical activity during postural perturbation is not well understood. These notions

115   altogether motivate the present work, wherein we report the employment of EEG to investigate the

116   cortical dynamics of postural adaptation and habituation with and without visual feedback following

117   vibratory proprioceptive stimulation of calf muscles.

2.   Material and Methods

2.1.   Experiment Setup

120   The main experiment was performed in the Icelandic Center for Neurophysiology at Reykjavik

121   University. Ten healthy subjects between 22 and 25 years old were instructed to maintain upright

122   posture during vibratory balance perturbations evoked by vibrators designed to deliver simultaneous

123   stimulation to both calf muscles. These vibrators comprised of revolving DC-motors equipped with a

124   3.5 g eccentric weight, contained in cylindrical casing measuring 0.06 m length and 0.01 m in diameter.

125   Each vibrator was held in place by elastic straps fastened tightly around the widest point of the calf

126   muscle, and electrical stimulation was set to deliver a vibratory amplitude of 1.0 mm and a vibration

127   frequency of 85 Hz. Stimulations were applied according to a pseudorandom binary sequence

128   schedule, where each shift had a random duration of 0.8 seconds to 6.4 seconds, yielding an effective

129   stimulus bandwidth of 0.1-2.5 Hz.

130   The subjects stood on a pressure platform where postural sway was monitored by recording anterio-

131   posterior and medial-lateral stance pressure changes [43]; it is important to note that although sway

132   and its corresponding EEG may be the product of the same perturbance, these responses are not

133   necessarily dependent upon each other. As such, postural sway was monitored here as a quality

134   control method to ensure appropriate stimulation response. Simultaneous to postural sway, EEG data

6

135   were recorded continuously from 64 channels in bipolar configuration, with each experimental trial

136   segmented into two phases lasting a total of 230 seconds: the quiet stance phase (30 seconds),

137   designated as the prestimulus baseline (BL), and the stimulation phase (200 seconds). Each stimulation

138   phase was subdivided into four segments, $Q1$-$Q2$-$Q3$-$Q4$, each containing 16 stimuli (64 in total per

139   experimental trial). In particular for this study, $Q1$ and $Q4$ segments were separately isolated to define

140   adaptation and habituation epoch events, respectively. Finally, experimental trials were performed

141   twice for each subject according to two conditions: with closed eyes (CE) and with open eyes (OE).

142   Experimental trial order was randomized for each subject in the cohort to reduce the effect of learning

143   due to repeated stimulus, as described [58].

2.2.   EEG Data Acquisition

145   The acquisition of EEG data was performed using a 64-channel wet-electrode cap in bipolar

146   configuration with a portable amplifier and recording tablet using EEGO software (ANT Neuro,

147   Enschede Netherlands). A standardized 10-20 system montage was used, and 3D head models were

148   generated with each subject in accordance with standard montage electrode positions [44]. After

149   strapping the calf muscle vibrators to both legs, participants were informed of the experiment

150   protocol, and the EEG cap was attached, followed by the application of conductive electrode gel to

151   reduce measured impedance to less than 10 kΩ in each channel. Next, a pair of bipolar electrodes were

152   placed proximal to each vibrator to isolate and define vibratory epochs for each stimulation phase.

153   After completing this instrumentation setup, the proprioceptive stimulation experiment was

154   initialized, with EEG data acquired at a sampling frequency of 512 Hz.

2.3.   Data Processing

156   Following data acquisition, recorded EEG was manually segmented for subject into OE and CE

157   recordings. Next, each dataset was processed according to a series of transformation operations to

158   prepare the measurements for analysis in a customized GUI in Matlab (MathWorks, Inc., Natick,

159   Massachusetts, USA). Initial preprocessing operations were performed as outlined:

1.   **Baseline and Stimulation Phase Extraction**: each baseline (BL) and stimulation phase which

160

161   were identified and extracted from each collected dataset to be separately processed.

162   2.   **Vibratory Stimuli Detection**: using the signal from both bipolar calf electrodes, each of the 64

163   experimental vibrations were manually identified and divided into their four segments, $Q1$-$Q2$

164   -$Q3$-$Q4$, as previously described. Subsequently, $Q1$ and $Q4$ segments were separately

165   extracted from the signal in order to describe:

166   a.   *Adaptation*: the initial effects evoked by the proprioceptive stimulation (BL vs. $Q1$).

167   b.   *Habituation*: the cortical conditioning process from prolonged postural perturbation

168   ($Q1$ vs. $Q4$)

169   3.   **Signal Filtering**: BL, $Q1$ and $Q4$ segments were filtered with a band-pass filter [0.3-80 Hz] with

170   a 24dB/octave roll-off to isolate six EEG frequency bands (Δ, 0.5-3.5 Hz; θ, 3.5-7.5 Hz; α, 7.5-

171   12.5 Hz; β, 12.5-30 Hz; γ_{low}, 30-50 Hz; and γ_{high}, 50-80 Hz). Moreover, signals were filtered

172   with a band stop filter from 49-51 Hz to remove undesired monomorphic artifacts from 50 Hz

173   mains electricity.

174   4.   **Artifact Detection**: automatic artefact detection using a manual voltage threshold set between

175   -100μV and +100μV was used to exclude segments contaminated by eye blinks and/or motion

176   artifacts. An artefact was detected automatically with the ASA feature "Artefact Detection", if

177   EEG data exceed threshold values in at least one channel. The user interfaces of the FFT

178   analysis features allow to "reject artefacts": this means that any events overlapping with

179   artefacts was not used in the respective feature. If thresholded detection was inadequate for

180   removing all visible artifacts, manual artefact identification was performed: all artefacts clearly

181   contaminated by motion artefacts were marked and then excluded from Fourier analyses.

182   Finally, the following series of postprocessing operations were then executed:

183   1. **Fast Fourier Transformation (FFT):** FFT processing of each EEG dataset was performed using

184   ASA software (ANT Neuro, Enschede Netherlands) using a frequency resolution of 0.977 Hz

185   [62], and epoch durations set to 30 seconds for BL data and the entire stimulus duration (as

186   previously noted, ranging from 0.8-6.4 seconds) for $Q1$ and $Q4$ stimulation datasets.

187   2. **Power Spectrum Extraction**: power spectral density (PSD) values and topologies were then

188   obtained from FFT analysis, normalized in ASA, and finally exported in ASCII format.

189   PSD values were exported in this regard for cohort comparison and statistical analysis using Matlab.

190   **2.4.   Power Spectra Variation**

191   As previously stated, the primary objectives of the present investigation were to analyze cortical

192   markers for OE and CE postural adaptation ($Q1 - BL$) and habituation ($Q4 - Q1$). To investigate these

193   differences and clarify the role of the cerebral cortex in postural control, OE and CE difference spectra

194   topologies were extracted for each EEG frequency band, showing electrodes and corresponding

195   cortical regions with significant differences in utilization. In this comparison, significant changes in

196   mean spectral power at each electrode were assessed using paired heteroscedastic t-tests, yielding

197   topological P-value maps for each EEG waveform (with $P < 0.05$ the threshold for significance).

198   Furthermore, spectral power variations ($\delta\%$) were calculated for the cohort to assess whether percent

199   changes in adaptation and habituation were significantly different depending on the availability of

200   visual feedback. To do this, PSD values were extracted and averaged within each band over all

201   electrodes, resulting in 6x1 vectors for each subject for both OE and CE trials, according to the following

202   expressions:

203   **Adaptation**: $\delta(Q1 - BL)\% = 100 \times \frac{\mu_{Q1} - \mu_{BL}}{\mu_{BL}}$ (1)

204   **Habituation**: $\delta(Q4 - Q1)\% = 100 \times \frac{\mu_{Q4} - \mu_{Q1}}{\mu_{Q1}}$ (2)

205   To assess statistical significance between datasets, pairwise, two-sample Z-tests were performed, and

206    $P < 0.05$ was analogously considered the threshold for significance. To account for multiple

207   comparisons, the P-values of sensor-wise comparisons were tested using the Benjamini–Hochberg

208   (BH) method [71], wherein the total number of tests (384) was calculated as the product of the number

209   of channels (64) and the number of frequency bands (6), considering adaptation and habituation as

210   separate test families.

2.5.   Power Spectra Linearity

212   To assess the degree of correlation between PSD values in each recording epoch, mean spectral values

213   for each member of the cohort were plotted against their own respective frequency band. For postural

214   adaptation analysis, BL and $Q1$ average values were compared for each frequency band, and for

215   habituation assessment, $Q4$ and $Q1$ PSD values were compared. Pearson's correlation coefficients, r,

216   were calculated for each correlation and were considered significantly correlated for $|r| > 0.7$ [63].

217   Furthermore, P-values were calculated using a homoscedastic, two-tailed Student's t-test of the null

218   hypothesis that there exists no linear relationship, with $P < 0.05$ the threshold for significance.

2.6.   Functional Connectivity Analysis

2.6.1.   Brain Network Construction

221   Functional brain networks were constructed using the "EEG source connectivity" method, which is

222   comprised of two main steps [45]: 1) reconstruction of cortical source dynamics by solving the inverse

223   problem, and 2) estimation of the functional connectivity between reconstructed signals. Here, we

224   used the weighted minimum norm estimate (wMNE) algorithm as the inverse solution [59]. The wMNE

225   was computed, using Brainstorm [68] toolbox for a cortical mesh of 15000 vertices using openMEEG

226   [69]. A Desikan-Killiany atlas-based segmentation approach was used, consisting in 68 cortical regions

227   [70]. Time series within one region of interest were averaged after flipping the sign of sources with

228   negative potentials. . Reconstructed regional time series were band-pass filtered across the six

229   reported EEG frequency bands. Next, functional connectivity between regional time series was

230   computed for each frequency band, using the phase locking value (PLV) metric, which returns a PLV

231   value between 0 (no phase locking) and 1 (full synchronization) [46, 47].

2.6.2.   Network Metrics

233   While functional connectivity provides key information about how different cortical regions are linked,

234   graph theory analysis (GTA) offers a framework to characterize the network topology and organization.

235   In practice, while many GTA metrics can be extracted from networks to characterize both local and

236   global properties, we report the utility of two, in particular:

237   1. **Network Segregation (Local Information Processing)**: The clustering coefficient, CC, was

238   computed as a direct measure of network segregation [64]. In brief, CC denotes how close a

239   node's neighbors tend to cluster together [65]. This coefficient is the proportion of connections

240   among a node's neighbors, divided by the number of connections that could possibly exist

241   between them, which is zero if no connections exist and one if all neighbors are connected.

242   2. **Network Integration (Global Information Processing)**: The relative importance of a node is

243   proportional to its betweenness centrality, C, which reflects the proportion of the number of

244   shortest paths in which the node participates (see [66] for a technical review).

245   All extracted network GTA measures were normalized with respect to random networks. Thus, we

246   generated 500 surrogate random networks, derived from the original network, by randomly

247   reshuffling the edge weights. Normalized values were computed by dividing original values by the

248   average values computed on the randomized graphs [48]. Finally, the Jonckheere-Terpstra test was

249   used to evaluate the trends of network GTA metrics as a function of the level of control (from BL to

250    $Q1$ through $Q4$). This non-parametric rank-based test can be used to determine the significance of a

251   trend by the computation of a z-score equivalent assembled against its critical value (with $P < 0.05$

252   the threshold for significance). The statistical difference between conditions was performed at the

253   level of each region (a node-wise analysis). Thus, the results are a set of brain regions that show

254   significant differences between the conditions.

3. Results and Discussion

3.1. Power Spectra Variation and Linearity

257   Our first PSD analysis method involved the topological comparisons of average spectral power values

258   for each EEG waveform, as well as their associated P-values to illustrate significant differences

259   between spectral power in individual electrodes; here, it is important to note that none of the P-values

260   from these comparisons resisted our BH correction procedure, and as such did not need correction.

261   **Figures 1-3** contain results from these analyses, showing comparisons between CE and OE conditions,

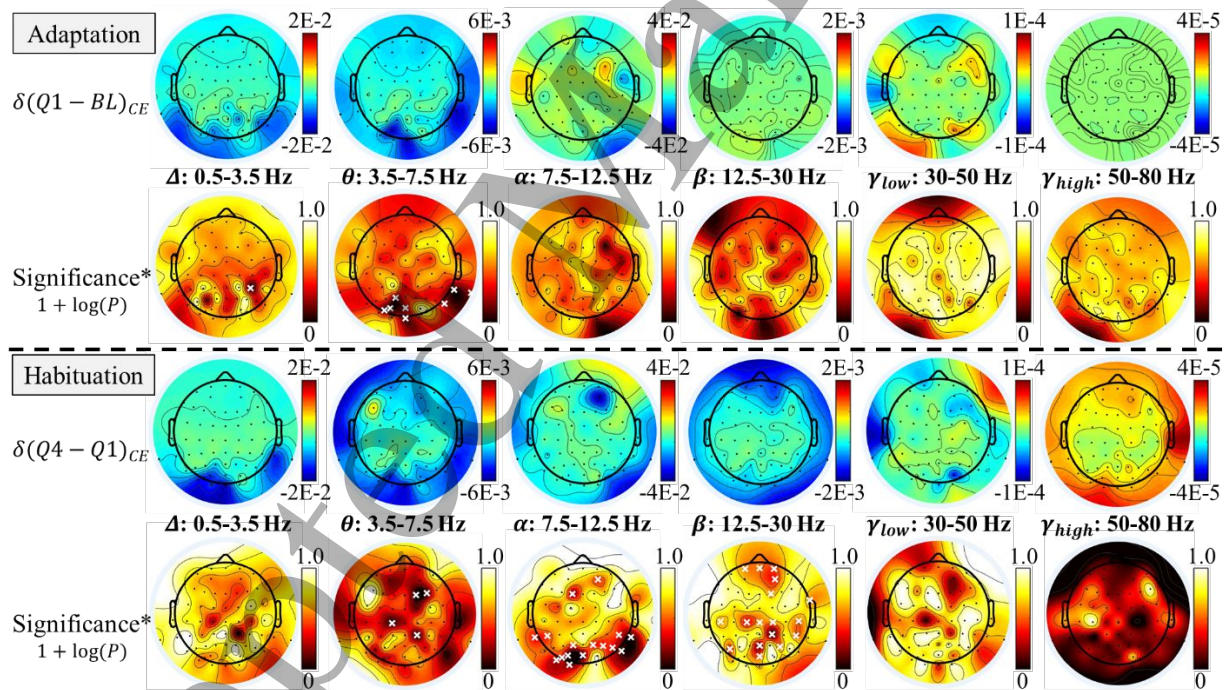262   in both adaptation ($Q1 - BL$) and habituation ($Q4 - Q1$).

264   **Figure 1**: Spectral topology differences during CE postural adaptation ($Q1 - BL$) and habituation (

265    $Q4 - Q1$). *Note statistical significance of $P < 0.05$ is denoted by each electrode denoted by a white

266   'x' in the significance maps.

267 As is evident in **Figure 1**, difference spectra values in CE adaptation varied considerably in specificity

268 to each EEG waveform, with a general reduction in $Q1$ spectral power over BL for lower frequencies

269 (Δ and θ), varied differences seen in α and β, and an increase in $Q1$ over BL in γ_{low} and γ_{high}. Significant

270 spectral differences from reduced $Q1$ power were highlighted in occipital and right-temporal Δ and θ.

271 Contrastingly, higher waveforms yielded more positive differences in spectral power; while not

272 significant, these differences may indicate a shift in cortical recruitment during CE postural adaptation

273 from lower to upper EEG waveforms. In habituation trials, difference spectra illustrated a nearly global

274 reduction in $Q4$ power over $Q1$, with the exception of γ_{high} and right frontal γ_{low}. Significant spectral

275 differences were found in θ around the precentral or superior frontal gyri, in addition to many

276 locations across the cortex in α and β bands; however, Δ, γ_{low}, and γ_{high} bands yielded minimal

277 significance. These results show a generalized decrease in cortical activity in CE postural habituation,

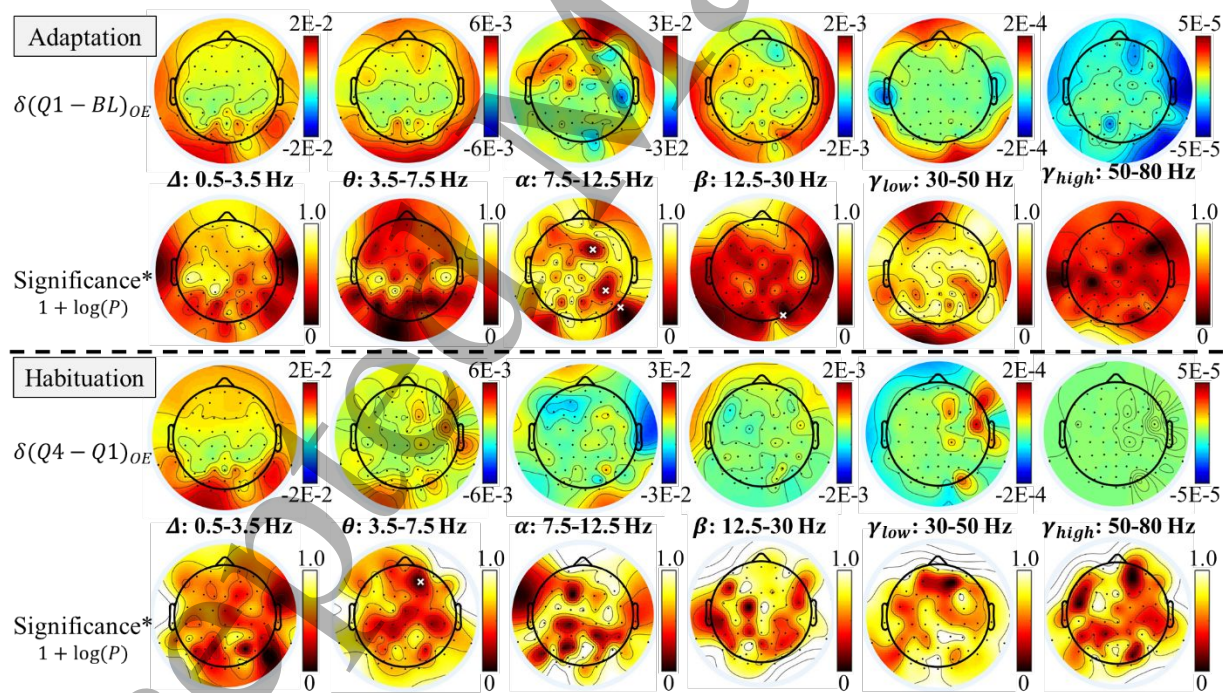278 suggesting the comparative activation of proprioceptive mechanisms over time.

279

280 **Figure 2**: Spectral topology differences during OE postural adaptation ($Q1 - BL$) and habituation (

281 $Q4 - Q1$). *Note statistical significance of $P < 0.05$ is denoted by each electrode denoted by a white

282 'x' in the significance maps.

283 As shown in **Figure 2**, OE adaptation difference spectra illustrated a nearly global increase in $Q1$ power

284 over BL, with the exception of γ_{high}. These results are directly antithetical to our findings in CE

285 adaptation, furthermore illustrating the inverse γ_{high} power relationship observed in CE habituation.

286 However, significant spectral differences (again uncorrected due to none resisting the BH correction)

287 from increased $Q1$ power were limited to right-temporal and occipital α and β. Nonetheless, these

288 results indicate that cortical recruitment may be directly related to the OE condition, as specifically

289 evidenced by the generalized increase in $Q1$ activity over BL. In habituation trials, difference spectra

290 again illustrated antithetical results to CE trials, showing an increase in $Q4$ power over $Q1$ in a majority

291 of channels for each EEG band. However, P-value topologies indicated only one significant electrode

292 in prefrontal θ, suggesting the necessity for additional comparisons to solidify implicated differences

293 between CE and OE trials (**Figure 3**).
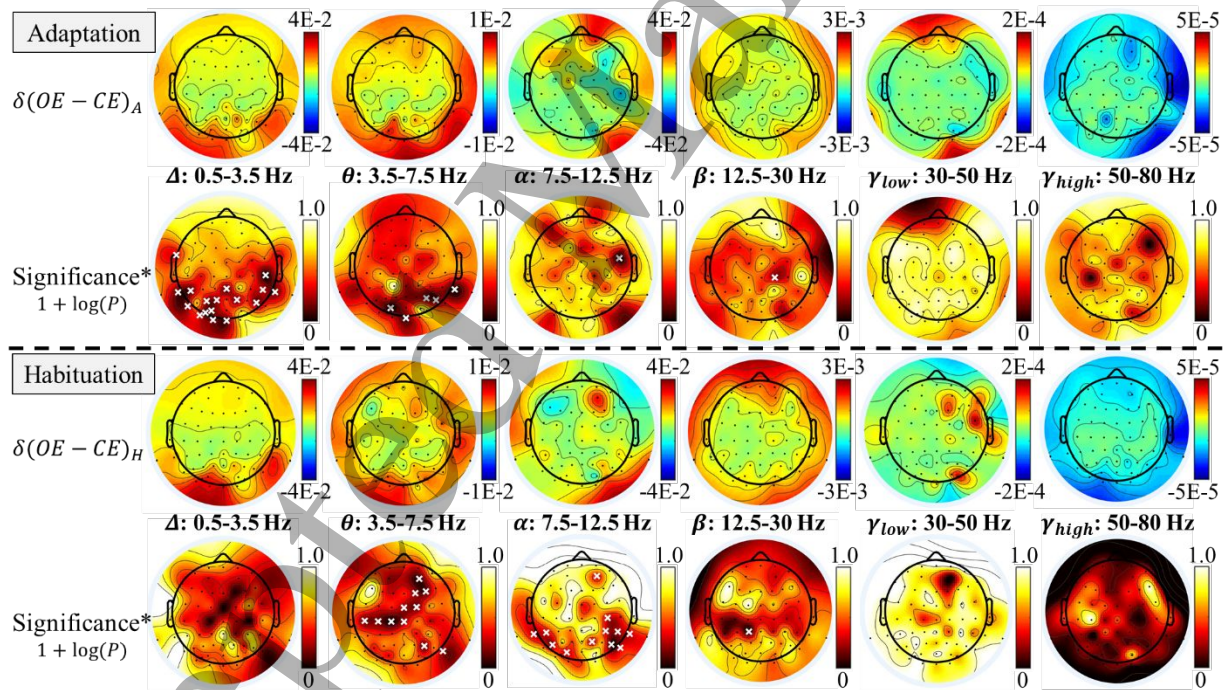

294

295 **Figure 3**: Spectral topology comparison between OE and CE difference spectra in both postural

296 adaptation and habituation. *Note statistical significance of $P < 0.05$ is denoted by each electrode

297 denoted by a white 'x' in the significance maps.

298   **Figure 3** depicts the comparison between OE and CE difference spectra, showing which trials incurred

299   more cortical activity in both adaptation and habituation. Since a majority of CE trials resulted in

300   negative spectral differences, while OE trials gave positive results (both in adaptation and habituation),

301   it is logical to expect a majority of these $\delta(OE - CE)$ values to be positive; indeed, this is precisely

302   what we observe. These differences are statistically significant in occipital and temporal electrodes for

303   Δ and θ bands during adaptation, with additional significant electrodes at the precentral gyrus in α

304   and β bands. Further significance during habituation is evident in θ at the left-precentral gyrus, as well

305   as the prefrontal and right-temporal cortices. Significance in habituation spectra was also found in the

306   α band through both occipital and right-posterior parietal electrodes. Finally, while again showing

307   fewer significant electrodes, habituation β differences yielded significance in one central parietal

308   electrode, with no significance in higher frequency waveforms. These results altogether show that the

309   disparate trends observed in OE and CE difference spectra are statistically significant, suggesting the

310   observation that cortical activity during postural control may be significantly higher with the use of

311   vision. These findings altogether directly support our hypothesis that visual recognition of instability

312   plays a critical role in governing the employment of cortical processes for postural control.

313   Following topological comparisons, pairwise spectral power variation ($\delta\%$) was calculated to assess

314   whether percent changes in adaptation and habituation were significantly different, depending on the

315   availability of visual feedback. The following tables contain results from this analysis, detailing the

316   pairwise, two-sample Z-tests with significance designated for $P < 0.05$ and $P < 0.01$ between CE and

317   OE adaptation and habituation trials.

318

319

320

321

Table 1. PSD pairwise variation in open eyes (OE) and closed eyes (CE) postural adaptation $(Q1 - BL)$ and habituation $(Q4 - Q1)$ spectral comparisons

	Frequency Band Pairwise Variation in Mean PSD[1]					
Adaptation:	$\boldsymbol{\Delta}$	$\boldsymbol{\theta}$	$\boldsymbol{\alpha}$	$\boldsymbol{\beta}$	$\boldsymbol{\gamma_{low}}$	$\boldsymbol{\gamma_{high}}$
$\delta(Q1 - BL)_{OE}$	83,5%	46,8%	13,0%	48,6%	11,9%	-93,1%[†]
$\delta(Q1 - BL)_{CE}$	-6,5%[†]	-30,9%[†]	-3,5%	-0,9%[†]	-8,2%	28,0%[†]
z-score	3,461**	0,729	0,772	2,472*	0,275	2,978**
Habituation:	$\boldsymbol{\Delta}$	$\boldsymbol{\theta}$	$\boldsymbol{\alpha}$	$\boldsymbol{\beta}$	$\boldsymbol{\gamma_{low}}$	$\boldsymbol{\gamma_{high}}$
$\delta(Q4 - Q1)_{OE}$	53,4%[†]	24,7%[†]	-2,3%	1,2%	12,8%[††]	35,2%[††]
$\delta(Q4 - Q1)_{CE}$	-36,6%	-31,6%	-20,8%	-43,9%	-3,7%	-13,4%
z-score	0,755	-0,343	-1,294	-2,285*	0,740	1,137

[1]Waveform bandwidths: Δ, 0.5-3.5 Hz; θ, 3.5-7.5 Hz; α, 7.5-12.5 Hz; β, 12.5-30 Hz; γ_{low}, 30-50 Hz; and γ_{high}, 50-80 Hz

z-test: *$P < 0.05$; **$P < 0.01$

Pearson's coefficient (linearity): [†]$R > 0.7$; [††]$R > 0.9$

322

323 The results presented in **Table 1** carry several important EEG waveform distinctions. Firstly, both OE

324 adaptation and habituation tests indicated an increase in spectral power across five of the six bands

325 (exceptions being γ_{high} and α, respectively), while CE tests resulted in decreases in power over all

326 habituation bands, along with all adaptation bands, except γ_{low}. These findings are in direct accordance

327 with the results shown in **Figures 1-3**, suggesting again that, following both acute and prolonged

328 proprioceptive perturbation, cortical activity is upregulated with the availability of visual feedback,

329 while conversely downregulated without vision. These notions further support our hypothesis that

330 visual recognition of instability plays a critical role in governing the employment of cortical processes

331 for postural control.

332 It is likewise intriguing to note both the significant difference between γ_{low} and γ_{high} values and the

333 degree of independence between γ_{low} and γ_{high} PSD values, overall. Extant literature has suggested

334 that generalized γ activity may precede the initiation of compensatory backward postural movement

335 when balance is in danger [29], but our results extend this notion with the segmentation of our γ

336 bands; it is evident here that the cortical response to instability with visual feedback engaged the γ_{low}

337 portion of the γ waveform, whereas the γ_{high} waveform was almost completely downregulated in

338 adaptation, yet upregulated with prolonged perturbation. Furthermore, antithetical to other bands,

16

339 γ_{high} spectral power increased significantly ($P < 0.01$) in CE adaptation trials, suggesting its specificity

340 as a cortical activity marker when vision is unavailable. However, it is important to likewise note that,

341 although these results present clear cortical differences between $Q1$ and $Q4$ which have are

342 referenced under the adaptation and habituation paradigm in literature [4], the onset of habituation

343 still remains differentially possible throughout the course of stimulation phases – a notion which

344 motivates further research in this regard.

345 In addition to the γ bands, the reported results likewise show the significant ($P < 0.05$) drop in β

346 waveform spectral power in both adaptation and habituation, but with strikingly disparate

347 characteristics. In adaptation, OE trials yielded a large upregulation in β, whereas CE trials yielded a

348 slight downregulation, suggesting again that vision is critical for governing cortical activation – most

349 significantly in high-frequency (γ and β) waveforms. However, in habituation, the OE β band remained

350 highly active, but dropped significantly ($P < 0.05$) in CE trials. This suggests again both the governing

351 role of the β waveform in visually-aided cortical postural control, along with its diminishing utility

352 without visual feedback.

353 Finally, the reported linearity results indicate some critical remarks regarding the degree of

354 dependence between each paired variable; however, it is first important to define our interpretation

355 of Pearson's correlation in this regard, wherein the greater the value of R, the lower the degree of

356 inter-bandwidth independence and the more any observed intra-bandwidth significance may be due

357 to natural spectral power variance. In adaptation, OE trials exhibited almost no linear correlation, with

358 the exception of γ_{high}, whereas CE trials exhibited significant ($R > 0.7$) linear dependence in all

359 bandwidths except α and γ_{low}. This distinction in comparing visual employment was antithetical in

360 habituation trials, wherein OE linear dependence was significant ($R > 0.7$) in Δ and θ bands and

361 strongly significant ($R > 0.9$) in both γ_{low} and γ_{high} bands, whereas CE trials yielded no linear

362 correlation. These results altogether suggest disparate levels of dependence upon cortical activation

363 when comparing OE and CE trials; in adaptation, the use of vision resulted in stronger inter-bandwidth

364 independence, whereas in habituation, this independence was stronger without vision.

365 **3.2.   Functional Connectivity Analysis**

366 Here, we explored two metrics for assessing functional connectivity during the three experimental

367 phases: brain network segregation (using clustering coefficients, CC) and network integration (using

368 betweenness centralities, C). The Jonckheere-Terpstra test was used to evaluate these network GTA

369 metrics as a function of the level of control (from BL to $Q1$ through $Q4$), with statistical significance

370 determined by z-score equivalence (with P-values of node-wise comparisons corrected analogously

371 using the BH false-discovery-rate method and $P < 0.05$ the threshold for significance). After

372 implementing this methodology, only θ-band segregation and α-band network integration yielded

373 statistical significance.

374 The top row in **Figure 4** shows CE network segregation cortical maps, denoting regions with a

375 significant increase in the θ band CC ($P < 0.05$, corrected) – a phenomenon mainly observed in central

376 regions (left precentral, left postcentral, right paracentral) and parietal regions (left and right

377 superioparietal). In addition, network integration maps illustrate a significant decrease in α -band

378 network integration ($P < 0.05$, corrected) from the experiment BL to stimulation phases $Q1$ through

379 $Q4$. These results mainly implicate cortical regions associated to the Default Mode Network (DMN: left

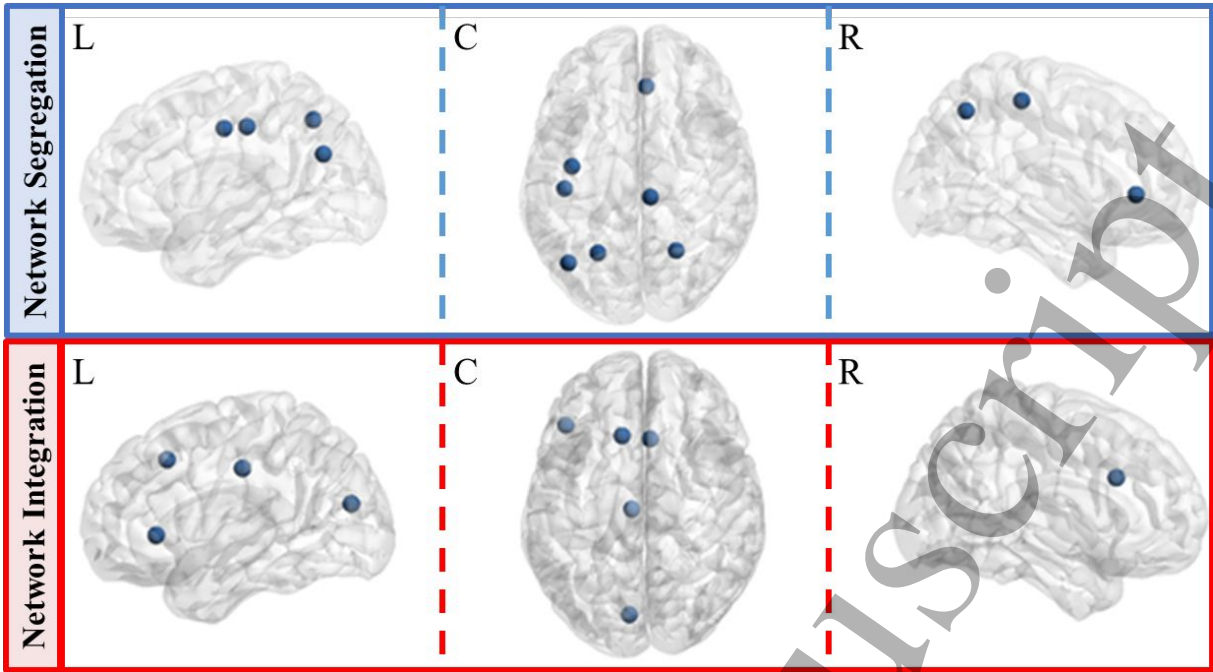380 anterior cingulate and left posterior cingulate), in addition to the cuneus and the left superiofrontal

381 regions.

18

382

Figure 4: 3D representation of cortical brain regions, showing network segregation differences from BL to $Q1$ to $Q4$ conditions within the θ band (top row) and network integration differences from BL, $Q1$ to $Q4$ conditions within the α band.

These results altogether indicate that cortical recruitment in postural control may be associated with decreased global functional connectivity at the θ band and decreased local functional connectivity at the α band. Before discussing the specific relevance of these findings, it is important to highlight the primary novelty of this type of investigation; this is the first reported employment of EEG source connectivity assessment to specifically characterize functional networks involved in postural control. While this notion makes it challenging to discuss the ultimate significance of these results, emerging literature does cite the utility of this method for investigating cognition [49] as well functional network changes in brain disorders [50], with correlative remarks to enable our discussion of this method in-context.

Our findings here suggest that functional brain networks are reshaped (i.e. undergo characteristic network modification) from a normative upright stance through perturbation in $Q1$ and $Q4$. This was most keenly expressed by the reported centro-parietal network's global characteristic shift in the θ

398   waveform; recent investigation into scalp-level EEG analysis from activity in this centro-parietal

399   network has reported similar changes from BL to task failure of a suprapostural motor task with

400   increasing postural destabilization [51]. The implication of parietal regions during postural control, in

401   particular, was also recently reported using functional near-infrared spectroscopy [52]. Furthermore,

402   frequency-based EEG source localization has implicated the θ band for its critical role in sensorimotor

403   control and sensory information processing [53]. Our reported increase in local θ connectivity may

404   therefore reflect activity occurring across the centro-parietal network that signifies either the planning

405   of corrective steps and/or precise cognitive analyses of potential biomechanical consequences from

406   incorrect or nonexistent postural correction.

407   Finally, the decrease in the α band network, located mainly in the DMN, may reflect an inhibition

408   phenomenon (well-known for the α band), wherein the key role of error detection within the cingulate

409   cortex was repressed – likely due to habituation [54, 55]. In addition, it was widely reported that the

410   α network is highly involved in attentional processes by enabling the inhibition of irrelevant networks,

411   influencing local/global signal processing, facilitating widespread information exchange, and

412   enhancing perception [56].

4. Conclusions

414   Human postural control is a complex physiological task, reliant upon adaptive feedforward and

415   feedback adjustments in the CNS, integrated with input from visual, vestibular, and somatosensory

416   systems. While the roles of the CNS and subcortical structures in postural control is well-documented,

417   there is still much debate in literature on the specific importance of the cerebral cortex and its

418   relationship with vison. This was the motivation for the present work, wherein we describe the use of

419   64-channel EEG to investigate power spectral changes and cortical dynamics during the vibratory

420   proprioceptive stimulation of calf muscles, measured with eyes open (OE) and eyes closed (CE).

421   The results presented here illustrate several principle conclusions. Firstly, power spectra variation

422   analysis showed waveform-dependent activation within cortical regions specific to postural adaptation

423   ($Q1 - BL$) and habituation ($Q4 - Q1$). In particular, the reported γ band segmentation extends

424   existing observations in literature that implicate its involvement in balance maintenance; we have

425   shown here that instability engaged γ_{low} and γ_{high} waveforms analogously in OE and CE postural

426   habituation, but the two bands behaved exactly the opposite in adaptation depending on the use of

427   vision. Furthermore, generalized spectral variation resulted in significant spectral power shifts (from

428   lower to higher frequencies) in CE adaptation trials, while generalized cortical activity decreased

429   significantly in CE habituation trials. OE trials showed the opposite phenomenon, with both adaptation

430   and habituation yielding increases in spectral power from BL to $Q1$ and $Q1$ to $Q4$, respectively – albeit

431   with fewer significant channels in each waveform. These results were further compared via pairwise

432   variation, which illustrated the significant nature of our OE and CE observations; however, power

433   spectra linearity results suggest that some EEG waveforms may not be strictly independent across trial

434   conditions.

435   An important limitation of this work lies in the present statistical comparison paradigm; as the use of

436   64 channels incurs the problem of multiple comparisons at the single-electrode level, P-value

437   correction may be needed, which typically employs methods for adjusting experimental α-levels for

438   significance (for example, using the Bonferroni correction [57], an adjusted single-voxel threshold

439   would be approximately: $\alpha = 0.05/(64^6) \cong 0.00013$). Achieving this level of significance at the single-

440   electrode level with the current experimental paradigm would require a prohibitively large sample

441   size; a problem which evidently correlates with increasing numbers of electrodes. For this reason,

442   controlling for the family-wise error rate may not be feasible for this type of study; instead, the BH

443   procedure to correct for false discovery rate is a useful method for addressing the probability of

444   incurring false positives. However, as none of our electrodes' spectral results resisted this correction,

445   we believe that the propensity of this study's strength lies instead in the pairwise variations and

446   functional connectivity results. Nonetheless, it is still important to observe significant spectral

447 difference topologies to identify potential cortical regions for future interrogation using higher spatial

448 resolutions.

449 We have additionally reported novel results that reveal potential cortical networks involved in postural

450 control using EEG source-space brain network mapping. Our reported increase in local θ connectivity

451 may signify either the planning of corrective steps and/or precise cognitive analyses of falling

452 consequences. In addition, α band network integration results may reflect an inhibition of error

453 detection within the cingulate cortex, likely due to habituation. Our findings here suggest that

454 functional brain networks undergo characteristic network modification; to our knowledge, these

455 findings present the first reported characterization of both local and global brain network reshaping

456 during postural control – a notion which necessitates future method optimization and the use of more

457 subjects to support these results.

458 Altogether, the present findings suggest the critical notion that, following both acute and prolonged

459 proprioceptive perturbation, cortical activity is upregulated with the availability of visual feedback,

460 while conversely downregulated without vision. However, conclusions on inter-bandwidth

461 independence would be strengthened by the use of more subjects, and implicated cortical regions

462 would be further strengthened by the use of higher spatial resolution EEG systems. Furthermore, it

463 should be made clear that the reported OE condition is a necessary but insufficient condition in itself

464 for directly relating these findings to the availability of visual input. In addition, future investigation

465 would be optimized by correlation with additional metrics for balance performance, such as

466 posturography or EMG to gauge postural sway. Results from these included metrics may indeed help

467 to clarify the feasibility and relevance of establishing the link between cortical response and body sway

468 analysis. Nonetheless, the present study illustrates novel EEG spectral comparisons that provide

469 evidence for the importance of visual referencing in postural control, and we further extend extant

470 research by the introduction of adaptive cortical response analysis. These results invoke a novel

471 emphasis on the importance of studying the role of the cortex in maintaining upright posture,

472   providing further insight on challenging questions from a range of fields, from neurorehabilitation to

473   the development of assistive tools for ambulation.

Disclosures

483   The authors declare that there is no conflict of interest regarding the publication of this paper.

Ethics Approval and Consent to Participate

485   Ethical approval for Icelandic subject data acquisition, as reported herein in this study, was obtained

486   by the Icelandic Science and Ethics Committee (RU Code of Ethics, cf. Paragraph 3 in Article 2 of the

487   Higher Education Institution Act no. 63/2006). All information regarding subject identity is

488   confidential in accordance with the "Act on the Protection of Privacy as regards the Processing of

489   Personal Data", No. 77/2000. All subjects have signed an informed consent agreement regarding

490   their participation and the anonymous publication of acquired data; consent forms were prepared

491   according to guidelines set by the Icelandic Bioethics Committee (Vísindasiðanefnd, Hafnarhæusið,

492   Tryggvagata 17, 101 Reykjavík Iceland) with approval reference ID 13-127-S1. No specific acquired

493   data will be made available to external entities, and any and all electronic data that may be

494   distributed between collaborating individuals is entirely anonymous.

5. References

[1] J. Satheesh Kumar and P. Bhuvaneswari, "Analysis of Electroencephalography (EEG) Signals and Its Categorization- A Study". In: Procedia Engineering 38, (2012) 2525 – 2536

[2] Niedermeyer E.; da Silva F.L. (2004). "Electroencephalography: Basic Principles, Clinical Applications, and Related Fields". Lippincott Williams & Wilkins. ISBN 0-7817-5126-8

[3] Bell, Martha Ann and Kimberly Cuevas (2012). "Using EEG to study cognitive development: issues and practices". In: Journal of cognition and development 13.3, pp. 281–294.

[4] Per-Anders Fransson (2005)."Analysis of adaptation in human postural control". Department of Otorhinolaryngology, Head and Neck surgery, Lund University, Sweden

[5] M. Pavol and Y. Pai, "Feedforward adaptations are used to compensate for a potential loss of balance". Exp Brain Res, vol. 145(4), pp. 528-538, 2002.

[6] D. Wolpert, Z. Ghahramani, and M. Jordan, "An internal model for sensorimotorintegration". Science, vol. 269(5232), pp. 1880-1882, 1995.

[7] Massion J. "Movement, posture and equilibrium: interaction and coordination". Prog Neurobiol. 1992; 38(1):35-56

[8] Massion, J. "Postural control system". Curr Opin Neurobiol 4, 877-87 (1994).

[9] J. Dichgans and H.-C. Diener, "The contribution of vestibulo-spinal mechanisms to the maintenance of human upright posture". Acta Otolaryngol (Stockh), vol. 107, pp. 338-345, 1989.

[10] T. Mergner and T. Rosemeier, "Interaction of vestibular, somatosensory and visual signals for postural control and motion perception under terrestrial and microgravity conditions--a conceptual model". Brain Res Rev, vol. 28(1-2), pp. 118-135, 1998.

[11] J. Massion, "Movement, posture and equilibrium: interaction and coordination". Prog Neurobiol, vol. 38(1), pp. 35-56, 1992.

[12] R. Johansson and M. Magnusson, "Human postural dynamics". CRC Crit Rev Biomed Eng, vol. 18, pp. 413-437, 1991.

[13] V. Dietz, "Human Neuronal Control of Automatic Functional Movements: Interaction Between Central Programs and Afferent Input". Phys Rew, vol. 72, pp. 33-69, 1992.

[14] Vette, A.H., Masani, K., Nakazawa, K., Popovic, M.R., 2010. Neural-Mechanical Feedback Control Scheme Generates Physiological Ankle Torque Fluctuation During Quiet Stance. IEEE Trans. Neural Syst. Rehabil. Eng. 18, 86–95.

[15] Butikov, E. I., On the Dynamic Stabilization of an Inverted Pendulum, American Journal of Physics 69,755- 768 (2001).

[16] Arinstein, A. and Gitterman, M., Inverted spring pendulum driven by a periodic force: Linear versus nonlinear analysis, European Journal of Physics 29,385- 392 (2008).

[17] Masani, K., V ette, A. H. and Popovic, M. R., Controlling balance during quiet standing: Proportional and derivative controller generates preceding motor command to body sway position observed in experiments, Gait & Posture 23,164-172 (2006).

[18] Fujisawa, N., Masuda, T., Inaoka, H., Fukuoka, Y., Ishida, A., Minamitani, H., 2005. Human standing posture control system depending on adopted strategies. Med. Biol. Eng. Comput. 43, 107–114.

[19] Mancini, M. et al. 2012. ISway: a sensitive, valid and reliable measure of postural control. J. NeuroEngineering Rehabil. JNER 9, 59–66.

[20] Ting, L. H. and McKay, J. L., Neuromechanics of muscle synergies for posture and movement, Current Opinion in Neurobiology 17, 622-628 (2007).

[21] Slobounova, S et al. Role of cerebral cortex in human postural control: an EEG study Clinical Neurophysiology 116 (2005) 315–323.

[22] Stoffregen, T. A. "Flow structure versus retinal location in the optical control of stance". J Exp Psychol Hum Percept Perform 11, 554-65 (1985).

[23] Tjernström, F. (2009). "Adaptation and learning in postural control". Department of Otorhinolaryngology, Lund University

[24] Brandt, T., Dichgans, J. & Koenig, E. "Differential effects of central verses peripheral vision on egocentric and exocentric motion perception". Exp Brain Res 16, 476-91 (1973).

[25] Straube, A., Krafczyk, S., Paulus, W. & Brandt, T. "Dependence of visual stabilization of postural sway on the cortical magnification factor of restricted visual fields". Exp Brain Res 99, 501-6 (1994).

[26] R. W. Baloh and V. Honrubia, "Clinical neurophysiology of the vestibular system". 2 edn ed. Philadephia: F.A. Davis Co, 1990.

[27] T. Roberts, "Reflex balance". Nature, vol. 244(5412), pp. 156-158, 1973.

[28] Hülsdünker T, Mierau A, Strüder HK. Higher Balance Task Demands are Associated with an Increase in Individual Alpha Peak Frequency. Frontiers in Human Neuroscience. 2015;9:695. doi:10.3389/fnhum.2015.00695.

[29] Slobounov S., Cao C., Jaiswal N., Newell K. M. (2009). Neural basis of postural instability identified by VTC and EEG. Exp. Brain Res. 199 1–16. 10.1007/s00221-009-1956-5

[30] Slobounov S. M., Teel E., Newell K. M. (2013). Modulation of cortical activity in response to visually induced postural perturbation: combined VR and EEG study. Neurosci. Lett. 547 6–9. 10.1016/j.neulet.2013.05.001

[31] L. Nashner, "Adaptation of human movement to altered environments". TINS, pp. 358-361, 1982.

[32] P. Brodal, "The central nervous system, structure and function". Oxford: Oxford university press, 1998.

[33] G. Goodwin, D. McCloskey, and P. Matthews, "Proprioceptive illusion induced by muscle vibration-Contribution by muscle spindles to perception". Science, vol. 175, pp. 1382-1384, 1972.

[34] van den Heuvel, M. P., & Hulshoff Pol, H. E. (2010). Exploring the brain network: a review on resting-state fMRI functional connectivity. European Neuropsychopharmacology : The Journal of the European College of Neuropsychopharmacology, 20(8), 519–534.

[35] Hassan, M., Dufor, O., Merlet, I., Berrou, C., & Wendling, F. (2014). EEG source connectivity analysis: from dense array recordings to brain networks. PloS One, 9(8), e105041.

[36] Welch, T. D. J., & Ting, L. H. (2014). Mechanisms of motor adaptation in reactive balance control. PloS One, 9(5), e96440.

[37] J. C. Eccles, "Learning in the motor system," presented at Prog Brain Res, 1986.

[38] J. Wolpaw, "Acquisition and maintenance of the simplest motor skill: investigation of CNS mechanisms". Med Sci Sports Exerc., vol. 26(12), pp. 1475-1479, 1994.

[39] Schmahmann, J. D. (2010). The role of the cerebellum in cognition and emotion: personal reflections since 1982 on the dysmetria of thought hypothesis, and its historical evolution from theory to therapy. Neuropsychology Review, 20(3), 236–260.

[40] T. Ledin, A. Kronhed, C. Möller, M. Möller, L. Ödkvist, and B. Olsson, "Effects of balance training in elderly evaluated by clinical tests and dynamic posturography". J Vestib Res, vol. 1(2), pp. 129-138, 1991.

[41] M. Hu and M. Woollacott, "Multisensory training of standing balance in older adults: I. Postural stability and one-leg stance balance". J Gerontol., vol. 49(2), pp. M52-61, 1994.

[42] G. Goodwin, D. McCloskey, and P. Matthews, "The contribution of muscle afferents to kinaesthesia shown by vibration induced illusions of movement and by the effects of paralysing joint afferents". Brain, vol. 95(4), pp. 705-748, 1972.

[43] Patel M, Gomez S, Lush D, Fransson PA (2009) Adaptation and vision change the relationship between muscle activity of the lower limbs and body movement during human balance perturbations. Clin Neurophysiol 120: 601–609.).

[44] G.E. Chatrian, E. Lettich, and P.L. Nelson. Ten percent electrode system for topographic studies of spontaneous and evoked EEG activity. Am J EEG Technol, 25:83-92, 1985.

[45] M Hassan, F Wendling. Electroencephalography Source Connectivity: Aiming for High Resolution of Brain Networks in Time and Space. IEEE Signal Processing Magazine 35 (3), 81-96, 2018.

[46] Lachaux, J. P., Rodriguez, E., Martinerie, J., & Varela, F. J. (1999). Measuring phase synchrony in brain signals. Human Brain Mapping, 8(4), 194–208.

[47] Kabbara, A., EL Falou, W., Khalil, M., Wendling, F., & Hassan, M. (2017). The dynamic functional core network of the human brain at rest. Scientific Reports, 7(1), 2936.

[48] Rubinov, M., & Sporns, O. (2010). Complex network measures of brain connectivity: uses and interpretations. NeuroImage, 52(3), 1059–1069.

[49] Ahmadlou, M., Gharib, M., Hemmati, S., Vameghi, R., & Sajedi, F. (2013). Disrupted small-world brain network in children with Down Syndrome. Clinical Neurophysiology : Official Journal of the International Federation of Clinical Neurophysiology, 124(9), 1755–1764.

[50] Brzezicka, A., Kaminski, J., Kaminska, O. K., Wolynczyk-Gmaj, D., & Sedek, G. (2017). Frontal EEG alpha band asymmetry as a predictor of reasoning deficiency in depressed people. Cognition & Emotion, 31(5), 868–878.

[51] Huang, C.-Y., Lin, L. L., & Hwang, I.-S. (2017). Age-Related Differences in Reorganization of Functional Connectivity for a Dual Task with Increasing Postural Destabilization. Frontiers in Aging Neuroscience, 9, 96.

[52] Karim, H., Fuhrman, S. I., Sparto, P., Furman, J., & Huppert, T. (2013). Functional brain imaging of multi-sensory vestibular processing during computerized dynamic posturography using near-infrared spectroscopy. NeuroImage, 74, 318–325.

[53] Sipp, A. R., Gwin, J. T., Makeig, S., & Ferris, D. P. (2013). Loss of balance during balance beam walking elicits a multifocal theta band electrocortical response. Journal of Neurophysiology, 110(9), 2050–2060.

[54] Anguera JA, Seidler RD, Gehring WJ. Changes in performance monitoring during sensorimotor adaptation. J Neurophysiol 102: 1868–1879, 2009

[55] Gehring W, Liu Y, Orr J, Carp J. The error-related negativity (ERN/Ne). In: The Oxford Handbook of Event-Related Potential Components, edited by Luck S, Kappenman E. New York: Oxford Univ. Press, 2012, p. 231–294.

[56] Sadaghiani, S. & Kleinschmidt, A. Brain Networks and alpha-Oscillations: Structural and Functional Foundations of Cognitive Control. Trends Cogn Sci 20, 805-817, doi:10.1016/j.tics.2016.09.004 (2016).

[57] Maris, E., & Oostenveld, R. (2007). Nonparametric statistical testing of EEG- and MEG-data. Journal of Neuroscience Methods, 164(1), 177–190.

[58] Adaptation to Vibratory Perturbations in Postural Control. Fransson PA et al, IEEE Engineering in Medicine and Biology Magazine 2003;22(2):53 – 57

[59] Adkin AL, Campbell AD, Chua R, Carpenter MG (2008) The influence of postural threat on the cortical response to unpredictable and predictable postural perturbations. Neuroscience Letters 435:120–125.

[60] Little CE, Woollacott M (2014) EEG measures reveal dual-task interference in postural performance in young adults. Experimental Brain Research 233:27–37.

[61] Slobounov S, Hallett M, Stanhope S, Shibasaki H (2005). Role of cerebral cortex in human postural control: an EEG study. Clin Neurophysiol 116(2):315-23.

[62] T. Hülsdünker, A. Mierau, C. Neeb, H. Kleinöder, and H. Strüder, "Cortical processes associated with continuous balance control as revealed by EEG spectral power," Neuroscience Letters, vol. 592, pp. 1–5, 2015.

[63] Zhang, J., Wei, J., Wang, B., Hong, J., & Wang, J. (2014). Nonlinear EEG decoding based on a particle filter model. BioMed Research International, 2014, 159486.

[64] Bullmore, E., and Sporns, O. (2009). Complex brain networks: graph theoretical analysis of structural and functional systems. Nature Reviews Neuroscience 10, 186-198.

[65] Watts, D. J., & Strogatz, S. H. (1998). Collective dynamics of "small-world" networks. Nature, 393(6684), 440–442.

[66] Rubinov, M., & Sporns, O. (2010). Complex network measures of brain connectivity: uses and interpretations. NeuroImage, 52(3), 1059–1069.

[67] Pascual-Marqui RD. (1999). Review of Methods for Solving the EEG Inverse Problem. International Journal of Bioelectromagnetism.

[68] Tadel, F., Baillet, S., Mosher, J.C., Pantazis, D., and Leahy, R.M. (2011). Brainstorm: a user-friendly application for MEG/EEG analysis. Computational intelligence and neuroscience 2011, 8.

[69] Gramfort, A., Olivi, E., Clerc, M., and Papadopoulo, T. (2010). OpenMEEG: opensource software for quasistatic bioelectromagnetics. Biomedical engineering online 9, 45.

26

656 [70] Desikan, R.S., Ségonne, F., Fischl, B., Quinn, B.T., Dickerson, B.C., Blacker, D., Buckner,
657   R.L., Dale, A.M., Maguire, R.P., and Hyman, B.T. (2006). An automated labeling system for
658   subdividing the human cerebral cortex on MRI scans into gyral based regions of interest.
659   Neuroimage 31, 968-980.
660 [71] Knyazeva, M. G., Jalili, M., Frackowiak, R. S., & Rossetti, A. O. (2011). Psychogenic seizures
661   and frontal disconnection: EEG synchronisation study. Journal of Neurology, Neurosurgery &
662   Psychiatry, 82(5), 505–511.